RPT-O-G0017

Optimization of Support Point Locations and Force Levels of the Primary Mirror Support System

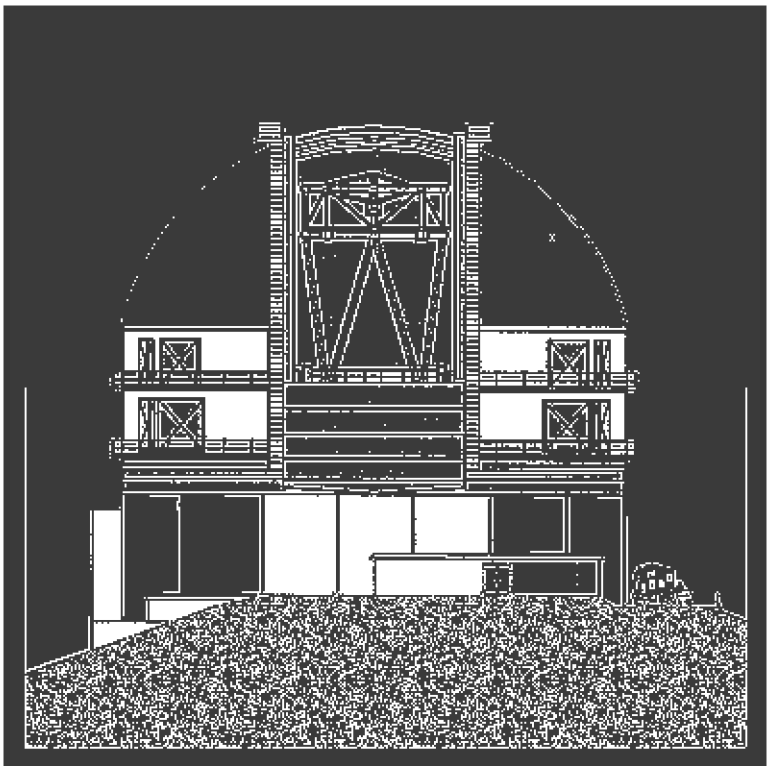

Myung K. Cho
Opto-structural Engineer

Ronald S. Price
Opto-mechanical Engineer

November 5, 1993

GEMINI PROJECT OFFICE 950 N. Cherry Ave. Tucson, Arizona 85719
Phone: (602) 325-9329 Fax: (602) 322-8590

GEMINI 8-M TELESCOPES PROJECT

Technical Report

Optimization of Support Point Locations and Force Levels of the Primary Mirror Support System

Myung K. Cho
Opto-structural Engineer

Ronald S. Price
Opto-mechanical Engineer

November 5, 1993

Table of Contents

I. EXECUTIVE SUMMARY

The Gemini Project has developed the pattern of support points located on the outer edge and rear surface of the primary mirror. It has also determined the force levels required at each of these support points.

In an effort to maximize producibility and minimize cost, the axial and lateral support actuators are constrained in position and force level, and the resulting residual errors in mirror figure are removed using active force correction. The axial support actuators are placed in five circular rings on the rear surface of the primary mirror and grouped into two force levels. The lateral support actuators are equally spaced around the edge of the mirror and also grouped into two force levels.

To analyze the support pattern locations and force levels, finite element models of the primary mirror were developed. Unit load cases were applied at each of the chosen support points in the model and these unit load cases were then combined into an influence matrix. Additional constraints related to the summation of forces and moments were placed on the influence matrix and then the mirror surface deformation was determined for each pattern of support points and forces.

After the axial and lateral support point locations and forces were individually determined, they were combined with the air pressure support, and total primary mirror system performance was calculated as a function of zenith angle. The distortions caused by the purely passive support were then corrected by the application of active optics forces at the axial supports. The resulting performance was quite good; a small application of active force provided a dramatic improvement in primary mirror surface figure, yielding essentially diffraction limited performance at 2.2 micrometers.

II. INTRODUCTION

The purpose of this report is to describe how the pattern of support points located on the outer edge and rear surface of the primary mirror and the level of force required at each one of these points were determined. These support points carry part of the weight, define the position and maintain the optical figure of the primary mirror over the operational range of zenith angles of the telescope. They are divided into two groups; those located on the rear surface of the primary are part of the axial support system and those on the outer edge are part of the lateral support system.

The axial support system is defined as those supports whose resultant force is parallel to the optical axis of the primary mirror. The lateral support system is defined as those supports

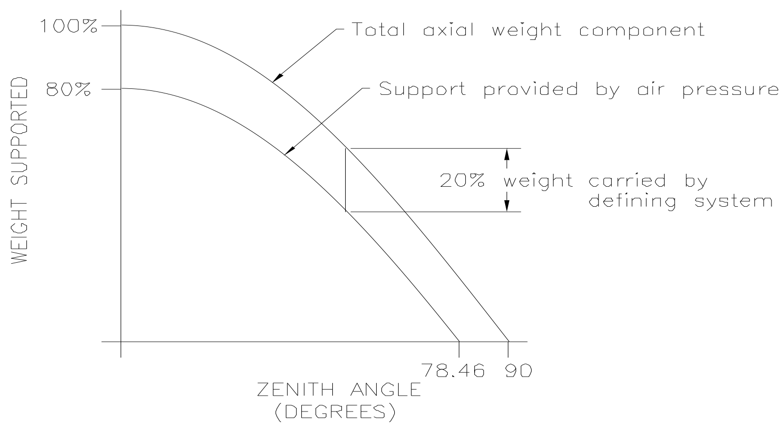

whose resultant force is perpendicular to the optical axis of the primary mirror. These definitions are important as neither the rear surface nor the outer edge of the primary mirror is normal to the optical axis of the telescope.

III. GENERAL DESCRIPTION OF PRIMARY MIRROR SUPPORT SYSTEM

Axial Support System

The total force provided by the axial support system varies as a function of the cosine of the zenith angle. At zenith pointing this force equals the full weight of the mirror, but at horizon pointing this force equals zero. Ideally, to minimize mirror deformation, the axial support system should provide a nearly uniform pressure over the entire back surface of the primary mirror. The uniform thickness and smooth, continuous back surface of the ULE™ primary mirrors make some form of fluid pressure support, e.g. air pressure, quite feasible. Seals can be installed at the inner and outer edges of the mirror and the air support pressure can be varied as a function of zenith angle to provide the desired force.

In addition to an air pressure support, a defining system of discrete points must be included to prevent mirror motion caused by external loads. It is advantageous for these defining points to carry part of the mirror weight as a preload: it minimizes slack and hysteresis that may occur at the zero-load condition, and it makes it possible to apply push-pull active optics forces without having to bond attachments to the mirror.

Therefore an axial support system was devised that consists of two parts: an air pressure part carrying approximately 80% of the mirror weight at the zenith pointing position and a defining part of 120 discrete points that carries the remaining 20% of the mirror weight. The air pressure required for support is low, approximately 3500 N/m^2 (0.5 psi), and is contained between the rear surface of the mirror and the top of the mirror cell by two annular seals at the outer edge and central hole of the primary mirror. These seals exert a small but non-negligible force on the mirror. This force is included in the optimization of the locations and force levels of the 120 axial defining points as discussed in a later section.

The active optics forces used to change the shape of the primary mirror will be superimposed on the nominal forces applied at these 120 defining points. Both push and pull active forces will be made possible by a supplemental bi-directional force actuator located directly beneath each support actuator and connected to it; the active force actuator will either add to, or subtract from the nominal force, depending on the direction of its force application.

As the telescope moves from zenith pointing toward horizon pointing the component of the mirror weight acting in the axial direction varies as the cosine of the zenith angle, therefore the axial support force must also vary in this way. One way to achieve this is to decrease both the air pressure and the forces provided by the 120 axial defining points in the same proportions as a function of zenith angle. However, a more effective method has been devised that reduces the air pressure more rapidly, allowing the forces at the 120 axial defining points to remain constant over the operational range of zenith angles (see Figure 1). This technique reduces hysteresis effects and the range of force required from the axial defining points during operation.

Figure 1. Rate of decrease of air pressure support as a function of zenith angle that maintains a constant force from the axial defining points.

A primary mirror that had a perfect optical figure in a zero gravity condition would exhibit small bumps on the optical surface when placed on the axial support system described here and subjected to the force of gravity. These bumps would be due to print-thru from the 120 axial defining points. However, the primary mirror will be supported, polished and tested on a system identical to the system hardware described here so these resulting bumps will be polished away along with all other surface imperfections, effectively 'marrying' the mirror to its support system. Because the force on the mirror provided by the 120 axial defining points does not vary with zenith angle, once the print through has been eliminated it will not reoccur at other zenith angles.

If, for any reason, the air pressure is lost during service, the full weight of the mirror will rest on the axial defining points. In this failure mode the primary mirror figure would exhibit print-thru in the optical surface; this effect will be described in a future report.

Lateral Support System

The total force provided by the lateral support system varies as the sin of the zenith angle. At zenith pointing this force is zero and increases to equal the full weight of the mirror at horizon pointing. As the zenith angle departs from zero, the supports along the lower half of the mirror's circumference must push up and those along the upper half must pull to keep the mirror from changing position or assuming an astigmatic shape.

Because of the previous analytical work in this area by ESO engineers, a lateral support system similar to that being used for the ESO VLT program has been adopted. The fundamental concepts for this approach are set forth in a paper by Schwesinger[1]. It utilizes a closed system of 72 passive hydraulic actuators around the outside edge of the mirror. None are placed in the central hole of the mirror as this area is completely filled by baffling and large field corrector assemblies. For practical reasons, it is desirable to make the lateral support points evenly spaced around the outside edge of the mirror.

Ideally, to minimize mirror deformation, the lateral support system should provide a nearly uniform support force around the periphery of the mirror and act through the center of gravity of the mirror. But, due to the curvature of the primary mirror, forces applied perpendicular to the optical axis to the edge of the mirror do not act through the center of gravity. Analysis has shown that these support forces must be applied at a compound angle to yield the desired result.

The forces in this arrangement will be applied through invar pads bonded to the edge of the mirror. The forces are applied at the centerline of the mirror's thickness and in a direction tangent to the surface curvature. To facilitate this, the edge of the mirror is made conical, perpendicular to the surface of the mirror at the edge. Due to the sensitivity of the angle of contact of the force applied to the edge of the mirror, 72 active axial force mechanisms are located at the edge of the mirror to 'trim' or compensate for any slight error in force direction.

IV. OPTIMIZATION STRATEGY FOR SUPPORT POINT LOCATIONS AND FORCE LEVELS

General

The manner in which the support point locations and force levels are determined and optimized is strongly dependent on the choice of design approach. The support point locations and force levels may be left unconstrained, allowing unique locations and force levels for each actuator. This level of design freedom would allow acceptable mirror figure performance over the operational zenith angle range of the telescope without the necessity of active optics force correction. Alternatively, constraints may be placed on the location and arrangements of the support point locations (confinement to circular rings, symmetry, etc.) and the force levels may be constrained to one or two groups in an effort to maximize producibility and minimize cost and maintenance of the support actuators. This latter approach requires a small amount of active force correction at each axial defining point to maintain required performance levels.

The theoretical performance of an unconstrained passive support system was analyzed. The locations and force levels of the axial defining points were allowed to vary independently; that is each point could have a unique location and force level. However, six-fold symmetry was placed on the axial defining points to comply with other design requirements. Refer to Gemini

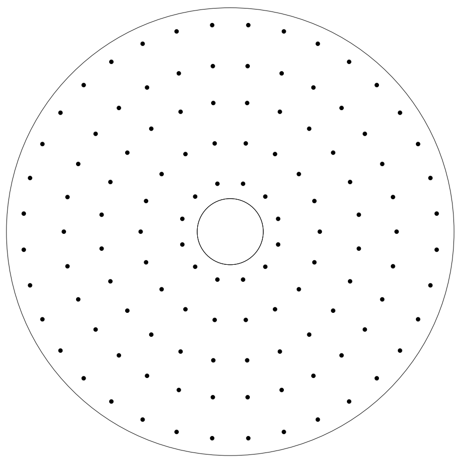

technical report, *The Distributed Defining System for the Primary Mirrors*.

The lateral support points were allowed to have unique force magnitudes and directions, but did retain equal spacing around the edge of the mirror and symmetry about the y-axis (left-right symmetry). The performance of this unconstrained system is quite good, maintaining primary mirror surface figure accuracy to within a few nanometers of the theoretically perfect surface over the operational range of zenith angles without active optics correction.

However, active optics forces are required to compensate for manufacturing errors, and the cost of uniquely different actuators would be prohibitive. Since active optics compensation is already a basic part of the design of the primary mirror support system, it makes sense to use a small part of this active optics force budget to simplify the support point locations, force levels and actuator design as long as mirror figure performance remains acceptable.

The following sections describe how the initial support point locations were determined and the optimization techniques used to improve upon them. The locations and forces of the 120 axial defining points were optimized separately from the locations and forces of the 72 lateral support points. Then the two were combined with the air pressure support to yield the performance of the complete primary mirror support system, as described in Section VI.

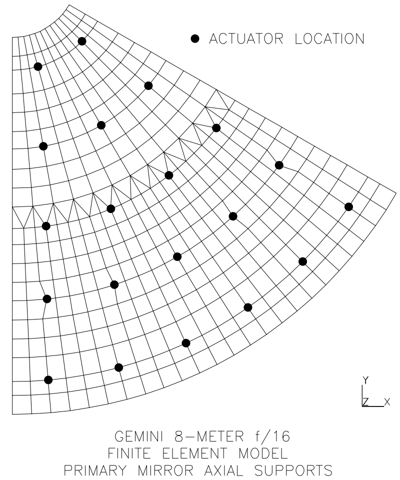

Figure 3. Finite element model used for analysis of the axial defining points

V. OPTIMIZATION PROCESS

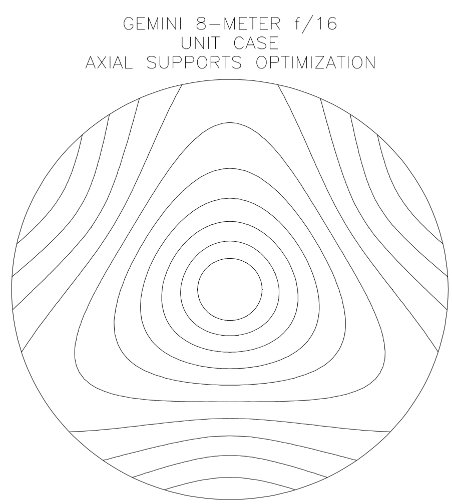

Figure 4. Intermediate unit load case generated during analysis.

Axial Defining Points

The initial layout of the locations of the 120 axial defining points was guided by the circular symmetry of the mirror and the requirement that each point support an approximately equal area of the mirror; hence all points would provide approximately the same force. This requirement was easily achieved because the uniform thickness and continuous back surface of the meniscus mirror allows the axial defining points to be located anywhere on the rear surface. This is an advantage compared to structured mirrors, which normally have support points located directly below the rib junctions[2]. It allows support point location, as well as force to be a variable during the optimization process.

To avoid asymmetric edge effects at the inner and outer edges of the mirror the defining points are configured in rings. The number of defining points per ring was taken from the number of equal diameter circles per ring in a close packed array. Because of the central hole, the first ring of twelve supports corresponds to the second ring in the array of circles. Initial analysis indicates that five support rings with 12, 18, 24, 30 and 36 support points respectively provided adequate support. This pattern is very similar to that employed by ESO for the VLT mirrors[3] and is shown in Figure 2.

Prior to optimization of axial defining point locations, the locations of the inner and outer seals for the air pressure support system were optimized. These seals act somewhat as axial support rings and their location affects the position of the support mechanism rings. It was determined that the best locations for the seals on the back of the mirror were as close as possible to the mirror edges.

Figure 2. Location pattern of the 120 axial defining points.

The force from these two air pressure seals was included in the optimization process. In addition, the force of gravity and a uniform support pressure equal to 80% of the mirror weight acting on the back of the mirror counter-acting gravity were included.

To analyze the support pattern locations and force levels, a one-sixth section finite element model was developed consisting of 384 shell elements and 405 nodes using Ideas™ software offered by Structual Dynamics Research Corporation running on a Sun Workstation. This model is shown in Figure 3.

The analysis started by applying unit loads at each of the twenty support points of the one-sixth model and determining their level of influence on the mirror surface figure. Unit loads included a normal direction force and moments about the x and y axes. Due to the six-fold symmetry of the pattern of 120 axial defining points, the results of these twenty groups of unit load cases can be extended to represent the full 120 axial support points on the back of the mirror. A plot of a unit load case is shown in Figure 4 as an example of an intermediate result during the process.

These unit load cases were then combined into what is called an influence matrix. The influence matrix is used to evaluate the effect of a change in force at each of the 120 axial defining points, or a change in support point location, or both, on the primary mirror surface figure. For the optimization, a least squares fit was used to determine the combination of the unit load cases that would meet the following requirements:

1) The summation of forces on the mirror provided by the 120 axial defining points equals 20% of the mirror weight.
2) The summation of moments about the center of the mirror equals zero.
3) The mirror surface deformation is minimized.

From the unconstrained case in which all forces and positions were allowed to vary independently we determined that the optimum force levels for the supports in the middle three rings were very similar, while the optimum force levels for the innermost ring were approximately 30% lower, and the optimum force levels for the outermost ring were

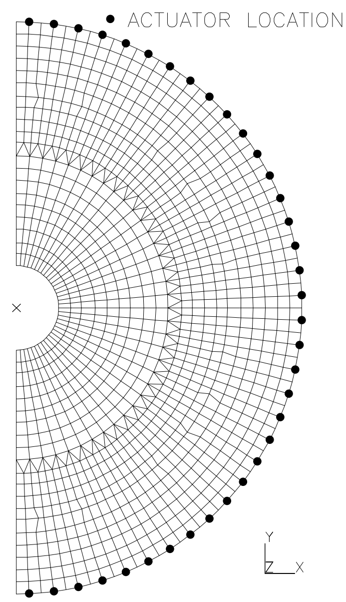

GEMINI 8–METER f/16
FINITE ELEMENT MODEL
LATERAL SUPPORTS OPTIMIZATION

approximately 3% lower. A decision was made to allow only two sizes of support mechanisms. It was further decided that for practical reasons the radial position of all actuators in each ring would be the same, and all actuators would be evenly spaced around the ring.

Two optimization cases were run. In the first, the radial position of each ring was allowed to vary, and the forces were constrained so that the supports in rings 2 through 5 had the same force, while the support forces in the innermost ring were identical but different than in rings 2 through 5. The second case was similar except the supports in rings 2 through 4 had the same force, while supports in rings 1 and 5 had a different force. Therefore, each optimization varied 5 ring radii and two force levels. The first optimization case gave the best results.

To evaluate a change in actuator position, a moment is placed at the original actuator position, rather than moving the position of the actuator in the model. This technique has been shown to be effective in evaluating the effect of a small change in position and thus prevents a constant rebuilding of the finite element model. Once the optimum support locations are determined, the finite element model is rebuilt to these final values and the design re-verified.

The optimization process has resulted in a passive axial support system that minimizes the amount of support print-thru with variations in air support pressure, the amount of active force correction necessary to establish and maintain the figure of the primary mirror during operation and the number of different axial support units. The axial supports are arranged in five rings with the following parameters:

Ring	**Radius (m)**	**Number of Axial Supports**	**Nominal Force (N)**
1	0.9005	12	285.6
2	1.6265	18	386.6
3	2.3554	24	386.6
4	3.0214	30	386.6
5	3.7633	36	386.6

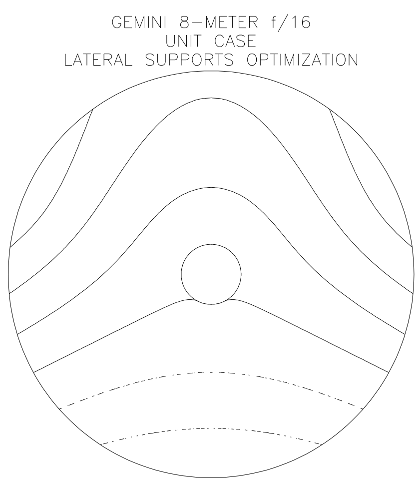

Lateral Support Points

The starting point was based on 72 lateral support points with the following constraints: 1) equal spacing along the periphery of the mirror, 2) magnitudes of the resultant forces would be placed into no more than two groups, 3) force vector directions were chosen to avoid interference between adjacent actuator assemblies and 4) the solution should not require corrective active forces at the axial defining points larger than 20 N.

The project was advised to include the effect of the attachment pads during the optimization process by engineers from the ESO VLT project, as the applied forces are slightly offset from the edge of the mirror due to the thickness of the support pad and introduce a bending moment.

To analyze the support locations and force levels, a one-half section model was developed consisting of 1152 shell elements and 1173 nodes using the same software and computer system as described in the axial support system section. This model is shown in Figure 5.

Figure 5. Finite element model used for lateral support system analysis

For the first design iteration, support forces were applied at the mid-plane of the mirror in the y direction only, with the mirror oriented in a horizon-pointing position. As optimization proceeded, the solution was improved by allowing the forces to be applied at a compound angle, with components in the x, y, and z directions. This required the calculation of 108 unit load cases (36 along each axis) and 72 unit moment cases (36 cases about the x and y axes) for the one-half model; employing symmetry these load cases were sufficient to model the full mirror with a total of 72 actuators. A plot of a unit load case is shown in Figure 6 as an example of an intermediate result during the process.

The unit load cases were combined to form an influence matrix. A least squares fit was used to determine the combination of the 72 unit load cases that would meet the following requirements:

1) The summation of forces in the y direction equals the weight of the mirror.
2) The summation of forces in the x direction equals zero.
3) The summation of forces in the z direction equals zero.
4) The mirror surface deformation was minimized.

From the unconstrained case in which all x, y, and z forces were allowed to vary independently we determined that the optimum force levels for the supports at the sides of the mirror were larger than the forces at the top and bottom. It was decided to allow only two sizes of support mechanisms, and a large number of different least-squares fit optimizations were performed to determine the support locations to put in each group.

Additional constraints were imposed in an interactive manner to ensure the orientations of the lateral support forces would avoid interference between the mechanisms and the edge of the mirror.

Figure 6. Intermediate unit load case generated during analysis.

The optimization process has resulted in support locations and forces for the lateral support system that meet the previously stated requirements. The 72 actuators are equally spaced, only two forces, 2752 N and 4086 N, are required, no interference exists between assemblies and the required active forces at the axial defining points are reasonable.

VI. SYSTEM PERFORMANCE AT VARIOUS ZENITH ANGLES

After the axial and lateral support point locations and forces were individually optimized, they were combined with the air pressure support and total primary mirror system performance was calculated as a function of zenith angle using the following relationship:

$$f(\theta) = (\cos\theta - 1)\,\Phi + (\sin\theta\,)\,\Psi$$

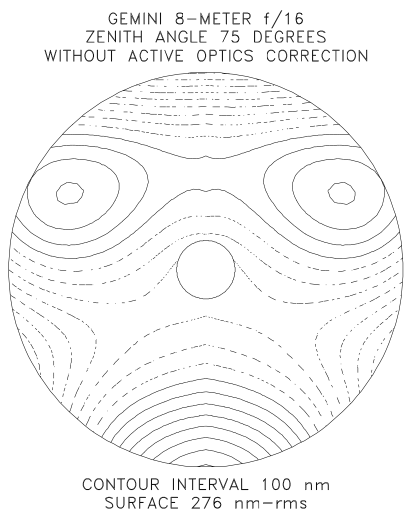

where Φ = distortion caused by axial air pressure support
Ψ = distortion caused by lateral support
θ = zenith angle

Primary mirror surface figure accuracy was computed at intervals of 15 degrees zenith angle and the distortions caused by the purely passive support were then corrected by active optics. Because the figure distortions are mostly low order, the level of improvement with only a small application of active force correction is dramatic; rms surface error of the primary mirror is decreased by a factor of fifty with the application of only 25 N maximum force at the axial support actuators. The residual rms errors after active optics correction meet the error budget for the primary mirror support system. The results are listed below:

Zenith Angle (degrees)	**f(θ) rms (nm) on passive support**	**Residual rms (nm) after active optics corrections**	**Maximum Active Force (Newtons)**
0	0	0	0
15	54	1.3	4.7
30	116	2.5	9.6
45	178	3.5	15.1
60	239	4.4	19.8
75	276	5.0	24.9
78	281	5.1	25.6

To reduce the data and provide a direct measure of imaging performance during optimization, a 64 x 64 grid file representing the optical surface of the mirror was used as input to Code V™ optical analysis software and encircled energy values were computed. These encircled energy values allow direct comparison between achieved performance and the allocated error budget for the axial support system. The optical imaging performance requirement for the telescope is very aggressive, but the allocated error budget for the total support system increases with increasing zenith angle.

An example of primary mirror surface figure performance is shown in Figure 7. The contour plot on the left shows the surface figure of the primary mirror prior to active optics correction at a zenith angle of 75°. The contour plot on the right shows considerable improvement with the application of active optics correction forces at the 120 axial defining points. The following table lists the diameters for encircled energy values of 50% and 85% at a wavelength of 2.2 micrometers for these two primary mirror surface profiles and compares them to a perfect or diffraction limited mirror.

	Diameter, arc-seconds	
Primary Mirror Surface Profile	**50%**	**85%**
Before active force correction	0.2390	0.4471
After active force correction	0.0652	0.1981
Diffraction limited	0.0651	0.1973

Figure 7. Primary mirror surface figure before and after active optics force correction at a zenith angle of 75°. Note the difference in contour intervals between the two plots.

VII. SUMMARY

Axial and lateral support point locations and forces have been designed and optimized that provide excellent performance over the operational zenith angles of the telescope. Of the 120 axial defining actuators, only two sizes are necessary in this design. Therefore performance has been maximized and cost and maintenance minimized. This level of performance requires only a small part of the available active optics force budget and should result in a cost effective and reliable mirror support system. The next step in the design process is a tolerance analysis of the support system to determine the sensitivity to various parameters such as actuator position, force level and air support pressure.

VIII. ACKNOWLEDGEMENTS

The authors wish to acknowledge the contributions made to this paper by Earl Pearson, Larry Stepp and Eugene Huang of the Gemini 8-M Telescopes Project

IX. REFERENCES

1. G. Schwesinger, "Lateral support of very large telescope mirrors by edge forces only", in Journal of Modern Optics, Vol. 38, No. 8, 1507-1516, (1991).

2. E. Pearson, L. Stepp, W. Keppel, "Support of 8-Meter Borosilicate Glass Mirrors", in Very Large Telescopes and their Instrumentation, M.H. Urich, ed., Proc. ESO Conference and Workshop No. 30, 435-449 (1988).

3. M. Schneermann, X. Cue, D. Enard, L. Noethe, H. Postema, "ESO VLT III : the support system of the primary mirrors", in Advanced Technology Optical Telescopes IV, SPIE Proceeding, Volume 1246, 920-928, (1990).

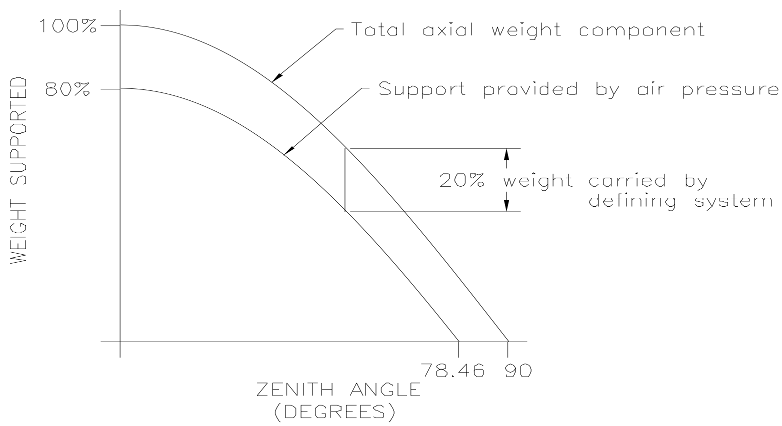
100%
80%
WEIGHT SUPPORTED
Total axial weight component
Support provided by air pressure
20% weight carried by
defining system
78.46
90
ZENITH ANGLE
(DEGREES)

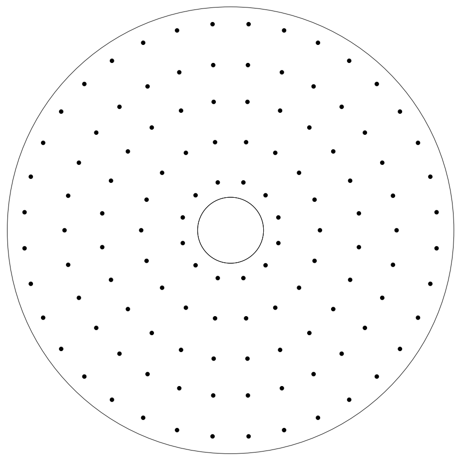

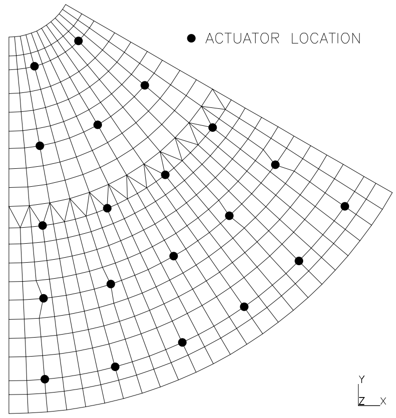

GEMINI 8–METER f/16
FINITE ELEMENT MODEL
PRIMARY MIRROR AXIAL SUPPORTS

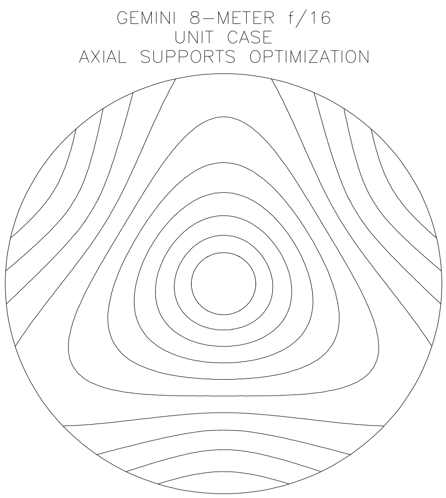
GEMINI 8-METER f/16
UNIT CASE
AXIAL SUPPORTS OPTIMIZATION

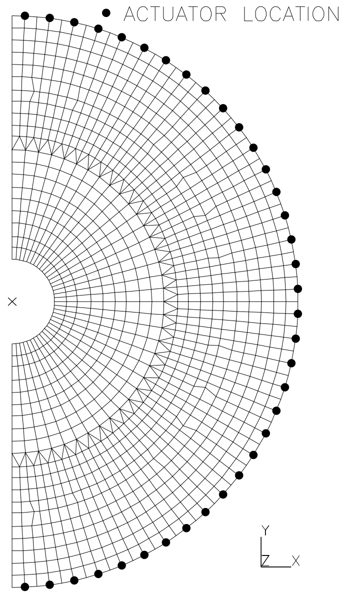

GEMINI 8–METER f/16
FINITE ELEMENT MODEL
LATERAL SUPPORTS OPTIMIZATION

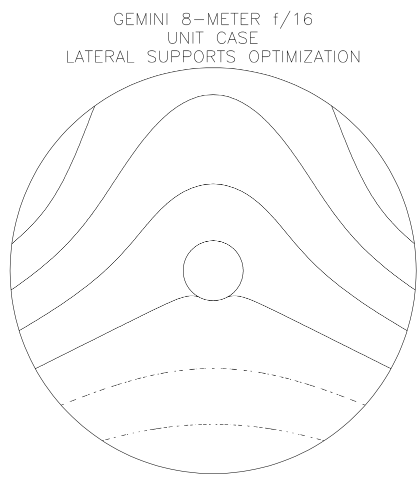
GEMINI 8-METER f/16
UNIT CASE
LATERAL SUPPORTS OPTIMIZATION

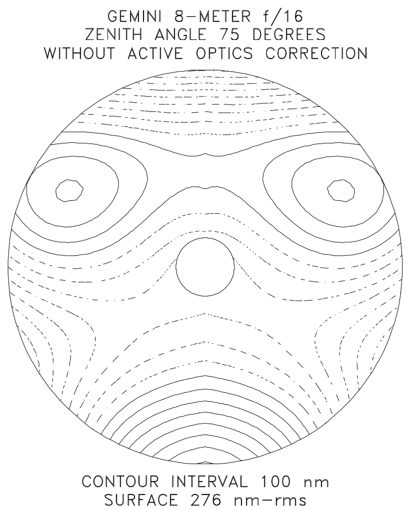
GEMINI 8-METER f/16
ZENITH ANGLE 75 DEGREES
WITHOUT ACTIVE OPTICS CORRECTION
CONTOUR INTERVAL 100 nm
SURFACE 276 nm-rms


GEMINI 8-METER f/16
ZENITH ANGLE 75 DEGREES
WITH ACTIVE OPTICS CORRECTION
CONTOUR INTERVAL 25 nm
SURFACE 40 nm-pv, 5 nm-rms